High speed and wide temperature range uncooled 1.3-μm ridge waveguide DFB lasers

Dingli Wang (王定理)[1,2,3*], Ning Zhou (周 宁)[2,3], Ruikang Zhang (张瑞康)[2,3], Xiaodong Huang (黄晓东)[2,3], Linsong Li (李林松)[2,3], Jun Zhang (张 军)[2,3], Shan Jiang (江 山)[2,3], and Jing Shi (石 兢)[1]

[1]*Department of Physics and Key Laboratory of Acoustic and Photonic Materials and Devices of Ministry of Education, Wuhan University, Wuhan 430072, China*

[2]*Accelink Technologies Co., Ltd., Wuhan Research Institute of Post & Telecommunications, Wuhan 430074, China*

[3]*State Key Laboratory for New Optical Communication Technologies and Networks, Wuhan 430074, China*

[*]*E-mail: dingli.wang@accelink.com*

Received December 12, 2008

A 1.3-μm wavelength vertical-mesa ridge waveguide mulitple-quantum-well (MQW) distributed feedback (DFB) laser with high directly modulated bandwidth and wide operation temperature range is reported. With the optimization of the strained-layer MQWs in the active region, the surrounding graded-index separated-confinement-heterostructure waveguide layers, together with the optimization of the detuning and coupling coefficient of the DFB grating, high directly modulation bandwidth of 16 GHz at room temperature and wide working temperature range from −40 to 85 °C are obtained. The mean time to failure (MTTF) is estimated to be over 2×10^6 h. The device is suitable as light source of high-bit-rate optical transmitters with small size and reduced cost.

OCIS codes: 140.5960, 230.5590, 250.5960.

doi: 10.3788/COL20090709.0809.

The demand on the high transmission bit-rate of optical local area network (LAN) and metropolitan area network (MAN) systems is getting stronger due to the worldwide popularization of Internet. High-speed directly modulated and wide temperature range distributed feedback (DFB) lasers are key components for LAN and MAN systems operating at 10 Gb/s and above, as they can be used as optical transceivers with reduced cost, small size, and low power consumption. Reduced cost requires that the DFB lasers can be directly modulated at high speed such as 10 Gb/s and above without external modulator. And it also requires that the laser material growth and structure design should be simple and easy. Small size and low power consumption require that the laser should work without Peltier cooler within a wide temperature range.

Previously, many literatures have reported the high speed directly modulated lasers in many material systems including InGaAsP, InGaAs/InGaAlAs/InP, and InGaAs/GaAs[1,2]. But the low cost criteria have not been addressed yet. Many reported designs with an InGaAsP active region favor a buried heterostructure or more exotic structures[1,3,4]. The extra growth and etch steps associated with these complicated structures increase the device cost and decrease its yield. Previously, we have reported high-speed directly modulated Fabry-Perot (FP) and DFB lasers with reversed-mesa ridge waveguide (RM-RWG) structure and polyimide planarization[5,6]. Although the RM-RWG structure together with polyimide planarization can surely increase the direct modulation bandwidth, this kind of structure is still complicated to manufacture as compared with vertical-mesa ridge waveguide (VM-RWG) structure.

In this letter, we report a 1.3-μm multiple-quantum-well (MQW) DFB laser with simple VM-RWG structure while maintaining high direct modulation bandwidth of 16 GHz at room temperature and wide working temperature range from −40 to 85 °C.

In order to simplify the manufacture process, the laser structure was designed with ordinary VM-RWG instead of RM-RWG to increase the device yield and accordingly reduce its cost. In order to realize the uncooled operation at high temperature, AlGaInAs material has been investigated as a promising candidate to improve temperature dependence of basic laser characteristics such as the threshold current and slope efficiency as its large conduction band offset[7]. Besides good temperature characteristics, AlGaInAs material system also has the advantage of realizing high speed modulation due to its high relaxation frequency by the higher differential gain compared with the conventional InGaAsP material system[8]. The key factor to realize high-speed directly modulated lasers is to improve the relaxation oscillation frequency (f_r) as well as reducing the device parasitic capacitance.

We optimized the structure of active region based on AlGaInAs strained MQW. In the design of the laser active region, large number of quantum wells is necessary to enhance the differential gain and reduce the gain saturation effect[9]. The active layer consisted of seven 5-nm-thick 1.3% compressively strained AlGaInAs quantum wells separated by 8-nm-thick slightly tension strained AlGaInAs barriers which were sandwiched in an AlGaInAs graded-index separated-confinement-heterostructure (GRIN-SCH). The photoluminescence (PL) wavelength of the active region was adjusted to

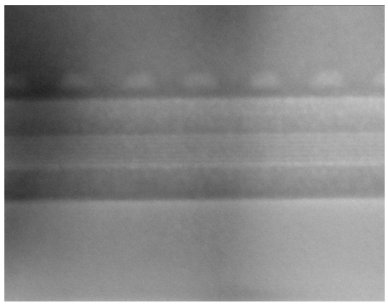

Fig. 1. SEM image of the MQW active region and floating grating of the LD.

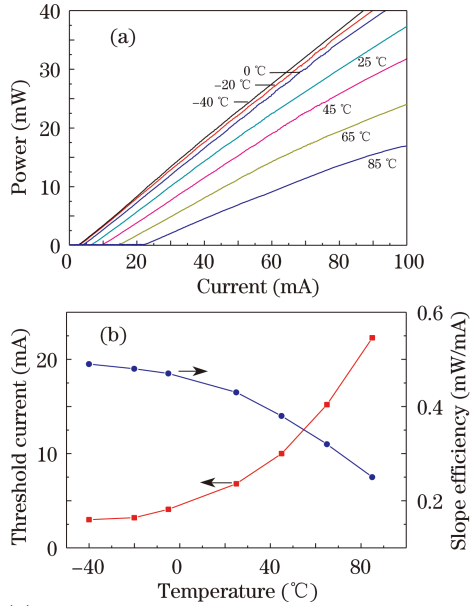

Fig. 2. (a) Output power versus current characteristics at different temperatures; (b) temperature dependence of the threshold current and slope efficiency of the LD.

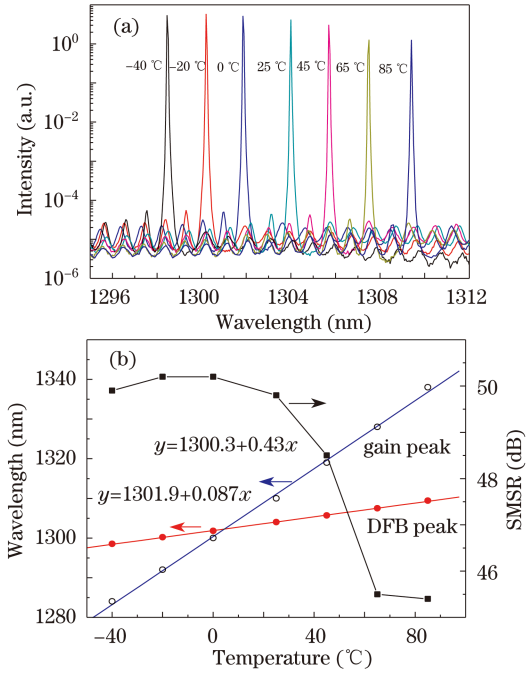

Fig. 3. (a) Longitudinal mode of the LD at different temperatures; (b) temperature dependence of the material gain peak, lasing wavelength, and SMSR of the LD.

around 1290 nm. The cladding layer consisted of a 50-nm-thick InAlAs layer and outer InP layers on both sides. The doping concentration of the InAlAs cladding layer was 3×10^{17} cm^{-3} for upper p-type and 1.5×10^{18} cm^{-3} for lower n-type regions, respectively. Narrow AlGaInAs SCH layer and InAlAs-cladding layers are also helpful for the lasers to realize large bandwidth.

The AlGaInAs MQW active layers and surrounding GRIN-SCH and cladding layers were grown onto the n-type InP substrate with low-pressure (70 torr) metal-organic chemical vapor deposition (MOCVD) growth technique. The laser structure was grown at 630 °C using H_2 as the carrier gas and TMIn, TEGa, TMAl, PH_3, and AsH_3 as source reactants for In, Ga, Al, P, and As respectively. Si_2H_6 and DEZn were used as source reactants for the Si and Zn dopants.

High performance (high speed and wide temperature range) DFB lasers require careful attention to be paid to the design and fabrication of the DFB grating, such as the grating structure, coupling coefficient, and wavelength detuning with respect to the material gain peak. Improved grating design can significantly enhance the laser performance, especially at higher modulation frequencies. An upper floating InGaAsP grating with bandgap energy wavelength of 1200 nm was grown to be above the etching-stop layer separated by a p-InP spacer layer. This upper floating grating structure is useful to reduce the injection current leakage and therefore lower the threshold current, and correspondingly raise the laser relaxation oscillation frequency at the same injection current. The grating was formed by low damage inductively coupled plasma (ICP) etching process using CH_4 and H_2 (1:5) gas mixture. By optimizing the grating depth and p-InP spacer thickness, we adjusted the kL product (coupling coefficient k multiplied by device length L) to be about 2.0. To further enhance the relaxation oscillation frequency while maintaining wide temperature performance of the laser diode (LD), the grating wavelength was slightly negatively detuned respect to the material peak gain at room temperature. The scanning electron microscopy (SEM) image of the MQW active region and floating grating is shown in Fig. 1.

After the regrowth of the grating-etched epitaxial wafer, it was processed into ordinary VM-RWG lasers, and the ridge width was restricted to be about 1.8 μm. The top electrode was fabricated using lift-off method, and the size of the electrode was shrunk to the minimum size of 80-μm diameter in order to reduce the parasitic capacitance. The completed wafers were then cleaved to a cavity length of 250 μm. High-reflection (HR, R=90%) and anti-reflection (AR, R=3%) coatings were formed on rear and front facets, respectively, to facilitate single-mode operation and enhance output power from the front AR coated facet. Laser chips were then mounted on AlN carriers with a junction-up configuration.

Figure 2(a) shows the characteristics of light output power versus bias current (P-I) at different temperatures from −40 to 85 °C. The threshold current ($I_{\rm th}$) and the slope efficiency are 7 mA and 0.45 mW/mA respectively at room temperature. At −40 °C, the threshold current is as low as 3 mA and the slope efficiency of more than 0.49 mW/mA is achieved. At the elevated temperature

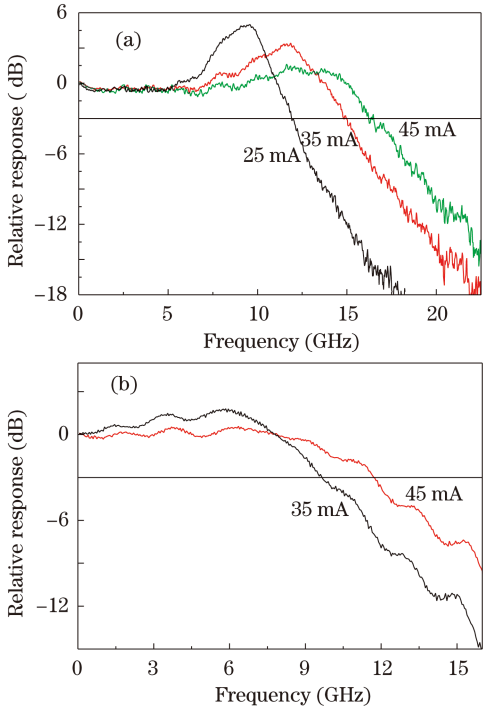

Fig. 4. Small signal frequency response of the LD at (a) 25 and (b) 85 °C.

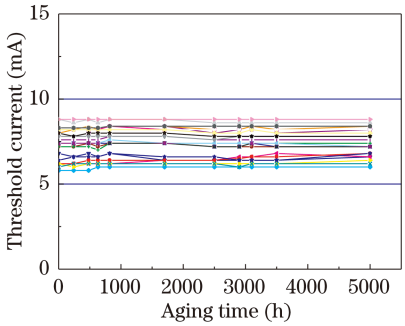

Fig. 5. Threshold current change versus aging time in ACC mode with aging condition of 100 °C and 100 mA for the lasers.

of 85 °C, the threshold current and the slope efficiency are respectively 22 mA and 0.25 mW/mA. High output powers over 40 and 15 mW at 100 mA are obtained at −40 and 85 °C, respectively. The variations of threshold current and slope efficiency versus temperature are shown in Fig. 2(b). It is shown that AlGaInAs laser has good temperature characteristic within the full temperature range from −40 to 85 °C.

Figure 3(a) shows the longitudinal mode of the LD in the full temperature range from −40 to 85 °C with a bias current of $I_{\rm th}(T)$+20 mA. The side mode suppression ratio (SMSR) and the lasing wavelength ($\lambda_{\rm c}$) together with the material gain peak are shown in Fig. 3(b). High SMSR of more than 45 dB is maintained within the whole measurement temperature range. The shift of the DFB lasing wavelength with temperature is only 0.09 nm/°C, while the material gain peak shift is about 0.43 nm/°C. The peak lasing wavelength at room temperature is about 6 nm negatively detuned from the material gain peak. At room temperature, the stop band is about 2 nm, consisting with the designed coupling coefficient. This is necessary for both the high speed modulation and the perfect temperature characteristic of the LD.

Figure 4(a) shows the typical small signal frequency responses at different bias currents measured at room temperature. The 3-dB bandwidth in excess of 16 GHz is achieved at the bias level of 45 mA. Figure 4(b) shows the small signal frequency responses at 85 °C. With a bias level of 45 mA, a 3-dB bandwidth of 12 GHz is achieved, and this is enough for 10-Gb/s uncooled direct modulation.

Figure 5 shows the profile of the threshold current change versus aging time in automatic current control (ACC) mode at 100 °C for the lasers. Stable operation for more than 5000 h has been maintained for all the 20 devices. The mean time to failure (MTTF) at room temperature, defined as the time for the threshold current to be increased by 50%, is estimated to be over 2×10^6 h. This MTTF value of conventional DFB laser with VM-RWG structure is more than that of laser with RM-RWG structure and polyimide planarization.

In conclusion, the 1.3-μm high-speed directly modulated wide working temperature range VM-RWG MQW DFB lasers for telecommunication applications are developed. By optimizing the structure of MQW active region and floating grating, large bandwidths of 16 and 12 GHz are achieved at room temperature and 85 °C, respectively. The threshold current and the slope efficiency are 7 mA and 0.45 mW/mA respectively at 25 °C. High reliability is confirmed by the aging test of ACC mode at 100 °C and 100 mA. The device is promising as light sources of 10-Gb/s optical transmitters with small size and reduced cost.

References

1. T. R. Chen, J. Ungar, X. L. Yeh, and N. Bar-Chaim, IEEE Photon. Technol. Lett. **7,** 458 (1995).
2. K. Czotscher, E. C. Larkins, S. Weisser, W. Benz, J. Daleiden, J. Fleissner, M. Maier, J. D. Ralston, and J. Rosenzweig, IEEE Photon. Technol. Lett. **9,** 575 (1997).
3. C. Kazmierski, A. Ougazzaden, D. Robein, D. Mathoorasing, M. Blez, and A. Mircea, Electron. Lett. **29,** 1290 (1993).
4. Y. Duan, T. Lin, C. Wang, F. Chong, and X. Ma, Chin. Opt. Lett. **5,** 585 (2007).
5. D. Wang, N. Zhou, J. Zhang, Y. Liu, N. Zhu, and L. Li, Chin. Opt. Lett. **3,** 466 (2005).
6. D. Wang, N. Zhou, J. Zhang, R. Zhang, X. Huang, L. Li, and J. Chang, Proc. SPIE **6020,** 60201U (2005).
7. N. Yamamoto, S. Seki, Y. Noguchi, and S. Kondo, IEEE Photon. Technol. Lett. **12,** 137 (2000).
8. J. C. L. Yong, J. M. Rorison, R. V. Penty, and I. H. White, in *Proceedings of CLEO 2001* CThL59 (2001).
9. H. Wada, K. Takemasa, T. Munakata, M. Kobayashi, and T. Kamijoh, IEEE J. Sel. Top. Quantum Electron. **5,** 420 (1999).